

The reassigned cross-spectrogram

Maria Åkesson
Centre for Mathematical Sciences
Lund University
Lund, Sweden
maria.akesson@matstat.lu.se

Julia Adlercreutz
Automatic Control
Lund University
Lund, Sweden
julia.adlercreutz@control.lth.se

Maria Sandsten
Centre for Mathematical Sciences
Lund University
Lund, Sweden
maria.sandsten@matstat.lu.se

Abstract—The reassignment technique is used to increase localization for signal components in the time-frequency representation. The technique gives perfect localization for linear chirp signals and constant frequency signals. Despite the recent interest in using the reassignment technique to determine phase-shifts, no general expression of cross-spectrogram reassignment vectors exists. This submission aims to give proof of the generalization of the reassignment vectors to the reassigned cross-spectrogram. The benefit of reassignment for determining phase shift between simulated signals will be illustrated. We exemplify with the reassigned cross-spectrogram of a respiratory frequency and a heart rate variability signal.

Index Terms—time-frequency, reassignment, instantaneous frequency, phase shift, multi-component

I. INTRODUCTION

The time-frequency (TF) reassignment and synchrosqueezing techniques are modern examples of representations that exploit the phase information usually discarded in the quadratic TF class. The reassigned spectrogram was first introduced in 1976 [1], and computationally efficient spectrogram reassignment vectors were introduced in 1995 [2]. In principle, the reassignment technique is a nonlinear transformation that moves TF mass in the spectrogram to improve signal localization. Importantly, the reassignment vectors can be interpreted as TF-local measures of the group delay and instantaneous frequency of the signal.

Over the past two decades, many more reassignment techniques have been suggested to overcome some of the limitations of reassignment, such as noise sensitivity and non-linear chirp and transient localization. Some notable mentions are, recursive versions of the reassigned spectrogram and scalogram [3], the adjustable Levenberg-Marquardt reassignment [4], reassignment including second-order phase-derivatives [5], scaled reassignment for transient signals [6], matched window reassignment [7], and noise-robust multitaper reassignment techniques. Similar to reassignment, synchrosqueezing is a nonlinear transformation of linear TF representations [8]. As such, it has become a popular tool for mode decomposition, [9], [10].

Phase shifts between signals are of interest in many fields, including direction of arrival estimation, source separation, and spatiotemporal decoding in neurology and soundscape analysis. The phase is often extracted from the short-time Fourier

transform or the cross-spectrogram. Other methods are based on bandpass-filtered signals and the Hilbert transform, which involves normalization of the signal by its own envelope. This procedure is well known to introduce spectral leakage and large errors into the phase measure [11].

To remedy this problem, we have suggested various reassignment methods based on the cross-spectrogram for determining phase shifts between transient signals [12], [13]. Another reassignment technique based on the cross-S-transform has been used for dispersion analysis of seismic waves [14]. The reassignment technique has also been applied for frequency-domain beamforming and cross-correlation estimation [15]. Phase estimation is also performed for speech signals by using filterbanks in combination with reassignment and synchrosqueezing techniques [16]. Despite the recent interest in using the reassignment technique to determine phase-shifts, no general expression of the cross-spectrogram reassignment vectors exists.

The contributions of this paper are threefold. First, we calculate the reassigned cross-spectrogram and give proof of the corresponding reassignment vectors. Second, we investigate the relation between the reassignment vectors and the short-time Fourier transform (STFT) phase. Lastly, we exemplify how the reassigned cross-spectrogram can be used to determine phase-shifts between frequency-modulated signals.

II. THE REASSIGNED CROSS-SPECTROGRAM

In correspondence with the ordinary reassigned spectrogram, we define the reassigned cross-spectrogram as

$$RS_{xy}^h(t, \omega) = \iint S_{xy}^h(\tau, \nu) \delta(t - \hat{t}_{xy}(\tau, \nu), \omega - \hat{\omega}_{xy}(\tau, \nu)) d\tau d\nu \quad (1)$$

where $x(t)$ and $y(t)$ are two signals. All integrals run from $-\infty$ to ∞ , and this is the case for all integrals in this work, unless something else is specified. The cross-spectrogram is most often complex-valued and is defined as

$$S_{xy}^h(t, \omega) = F_x^h(t, \omega) \overline{F_y^h(t, \omega)} \quad (2)$$

where \overline{F} denotes complex conjugate and

$$F_x^h(t, \omega) = \int x(u) \overline{h(t - u)} e^{-i\omega u} du \quad (3)$$

Thanks to Assoc. Prof. Peter Jönsson, Kristianstad University, Sweden, for sharing the heart rate variability data.

is the short-time Fourier transform (STFT) of the signal x using the window h . The purpose of the reassignment vectors $\hat{t}_{xy}(\tau, \nu)$ and $\hat{\omega}_{xy}(\tau, \nu)$ is to move the energy of the cross-spectrogram $S_{xy}(t, \omega)$ to the gravitational center.

We define the reassignment vectors for the cross-quadratic class as

$$\hat{t}_{xy}(t, \omega) = t - \frac{\iint u \phi(u, \nu) W_{xy}(t - u, \omega - \nu) du \frac{d\nu}{2\pi}}{\iint \phi(u, \nu) W_{xy}(t - u, \omega - \nu) du \frac{d\nu}{2\pi}} \quad (4)$$

and

$$\hat{\omega}_{xy}(t, \omega) = \omega - \frac{\iint \nu \phi(u, \nu) W_{xy}(t - u, \omega - \nu) du \frac{d\nu}{2\pi}}{\iint \phi(u, \nu) W_{xy}(t - u, \omega - \nu) du \frac{d\nu}{2\pi}} \quad (5)$$

where the cross-Wigner-Ville distribution is defined as

$$W_{xy}(t, \omega) = \int x\left(t + \frac{\tau}{2}\right) \bar{y}\left(t - \frac{\tau}{2}\right) e^{-i\omega\tau} d\tau. \quad (6)$$

The cross-Wigner-Ville distribution simplifies to the regular version if the two signals are the same. Similarly, the cross-quadratic class is defined as

$$W_{xy}^Q(t, \omega) = \iint \phi(u, \nu) W_{xy}(t - u, \omega - \nu) du \frac{d\nu}{2\pi}, \quad (7)$$

where $\phi(u, \nu)$ is the smoothing kernel. Again, it can be noted that, if the two signals are the same, the cross-quadratic class simplifies to the standard quadratic class.

Unfortunately, these expressions are not very useful for the cross-spectrogram since they require a lot of computing power. We want to find easy-to-compute expressions for the cross-spectrogram, using the STFT of signals and windows.

A. The cross-spectrogram

The cross-spectrogram belongs to the cross-quadratic class which can be seen from the following lemma.

Lemma 1. *Given two signals x and y , and two windows g and h*

$$F_x^g(t, \omega) \bar{F}_y^h(t, \omega) = \iint W_{gh}(u, \nu) W_{xy}(t - u, \omega - \nu) du \frac{d\nu}{2\pi} \quad (8)$$

Proof is found in Appendix. From Lemma 1 it follows that the cross-spectrogram is part of the cross-quadratic class with smoothing kernel

$$\phi(u, \nu) = W_{hh}(u, \nu)$$

It is also worth noting that the order of the signals in the cross-Wigner-Ville distribution matters, which is shown in the following lemma.

Lemma 2. *Given two signals x and y , switching the order of the signals in the cross-Wigner-Ville distribution is the same as taking the complex conjugate, i.e.*

$$W_{xy}(t, \omega) = \overline{W_{yx}(t, \omega)} \quad (9)$$

Proof. With x and y switched in (6) the right hand side of the equality is

$$\begin{aligned} \overline{W_{yx}(t, \omega)} &= \int \bar{y}\left(t + \frac{\tau}{2}\right) x\left(t - \frac{\tau}{2}\right) e^{i\omega\tau} d\tau \\ &= - \int \bar{y}\left(t - \frac{\hat{\tau}}{2}\right) x\left(t + \frac{\hat{\tau}}{2}\right) e^{-i\omega\hat{\tau}} d\hat{\tau} = W_{xy}(t, \omega) \end{aligned}$$

using $\hat{\tau} = -\tau$. □

B. Reassignment vectors

Now that all necessary notions have been defined, the main result of the paper follows.

Theorem 1. *The reassignment vectors for the cross-spectrogram can be computed as*

$$\hat{t}_{xy}(t, \omega) = t - \frac{1}{2} \left(\frac{F_x^{th}(t, \omega)}{F_x^h(t, \omega)} + \frac{\overline{F}_y^{th}(t, \omega)}{\overline{F}_y^h(t, \omega)} \right) \quad (10)$$

$$\hat{\omega}_{xy}(t, \omega) = \omega - \frac{i}{2} \left(\frac{F_x^{\frac{dh}{dt}}(t, \omega)}{F_x^h(t, \omega)} - \frac{\overline{F}_y^{\frac{dh}{dt}}(t, \omega)}{\overline{F}_y^h(t, \omega)} \right) \quad (11)$$

where F_x^{th} and $F_x^{\frac{dh}{dt}}(t, \omega)$ are the STFTs where $t \cdot h(t)$ and $dh(t)/dt$ are used as windows, respectively.

Proof. Firstly, the reassignment in the time domain will be shown and we start from the expression in (4). The denominator is easily found to be $F_x^h(t, \omega) \overline{F}_y^h(t, \omega)$ from Lemma 1. Next, it will be shown that the numerator can be written as

$$\frac{1}{2} \left(F_x^{th}(t, \omega) \overline{F}_y^h(t, \omega) + F_x^h(t, \omega) \overline{F}_y^{th}(t, \omega) \right).$$

The first step is to apply Lemma 1 on both terms in the equation above. This results in

$$\begin{aligned} &\frac{1}{2} \iint W_{h,th}(u, \nu) W_{xy}(t - u, \omega - \nu) du \frac{d\nu}{2\pi} + \\ &\frac{1}{2} \iint W_{th,h}(u, \nu) W_{xy}(t - u, \omega - \nu) du \frac{d\nu}{2\pi} \end{aligned}$$

Now Lemma 2 can be used to rewrite the expression to

$$\begin{aligned} &\frac{1}{2} \iint (W_{h,th}(u, \nu) + \overline{W}_{h,th}(u, \nu)) W_{xy}(t - u, \omega - \nu) du \frac{d\nu}{2\pi} \\ &= \frac{1}{2} \iint 2\Re(W_{h,th}(u, \nu)) W_{xy}(t - u, \omega - \nu) du \frac{d\nu}{2\pi} \end{aligned}$$

where \Re represents the real part. From [2] it is known that

$$\Re(W_{h,th}(u, \nu)) = u W_{hh}(u, \nu),$$

which means that the reassignment vector in (4) can be written as

$$\hat{t}_x(t, \omega) = t - \frac{1}{2} \frac{F_x^{th}(t, \omega) \overline{F}_y^h(t, \omega) + F_x^h(t, \omega) \overline{F}_y^{th}(t, \omega)}{F_x^h(t, \omega) \overline{F}_y^h(t, \omega)},$$

which further simplifies to (10).

The derivation for the frequency reassignment is very similar. The main difference is the fact that

$$\Im \left(W_{h, \frac{dh}{dt}}(u, \nu) \right) = -\nu W_{hh}(u, \nu),$$

known from [2], where \Im represents the imaginary part. Because the expression now contains the imaginary part instead of the real part, there will be a subtraction between two terms instead of an addition. With this, it can be shown that the numerator of the reassignment vector in (5) is equal to

$$\frac{i}{2} \left(F_x^{\frac{dh}{dt}}(t, \omega) \bar{F}_y^h(t, \omega) - F_x^h(t, \omega) \bar{F}_y^{\frac{dh}{dt}}(t, \omega) \right).$$

This means that the reassignment vector in (5) can be written as

$$\hat{\omega}_{xy}(t, \omega) = \omega - \frac{i}{2} \frac{F_x^{\frac{dh}{dt}}(t, \omega) \bar{F}_y^h(t, \omega) - F_x^h(t, \omega) \bar{F}_y^{\frac{dh}{dt}}(t, \omega)}{F_x^h(t, \omega) \bar{F}_y^h(t, \omega)}$$

which can be simplified to (11). \square

It can be noted that, if the two signals are the same, then the reassignment vectors for the cross-spectrogram simplify to those of the spectrogram.

C. Relation to STFT phase and magnitude

However, the cross-spectrogram reassignment vectors in (10) and (11) are complex-valued, which means that they cannot be used as TF coordinates in (1) directly. In this section, we investigate the interpretation of the real and imaginary parts of the reassignment vectors of the cross-spectrogram.

Let $M_x^h(t, \omega) = |F_x^h(t, \omega)|$ and $\Phi_x^h(t, \omega) = \arg(F_x^h(t, \omega))$ be the magnitude and phase of the STFT, respectively. Then, it is known from [17] that

$$\frac{F_x^{th}(t, \omega)}{F_x^h(t, \omega)} = t + \frac{\partial \Phi_x^h(t, \omega)}{\partial \omega} - i \frac{\partial}{\partial \omega} \log M_x^h(t, \omega) \quad (12)$$

$$\frac{F_x^{\frac{dh}{dt}}(t, \omega)}{F_x^h(t, \omega)} = \frac{\partial}{\partial t} \log M_x^h(t, \omega) + i \frac{\partial \Phi_x^h(t, \omega)}{\partial t}, \quad (13)$$

where $\frac{\partial}{\partial t}$ and $\frac{\partial}{\partial \omega}$ denotes the partial derivative with respect to t and ω , respectively. Inserted into (10) and (11), the reassignment vectors can be expressed in terms of the STFT phases and magnitudes, resulting in

$$\begin{aligned} \hat{t}_{xy}(t, \omega) = & - \frac{\frac{\partial}{\partial \omega} \Phi_x^h(t, \omega) + \frac{\partial}{\partial \omega} \Phi_y^h(t, \omega)}{2} \\ & + \frac{i}{2} \frac{\partial}{\partial \omega} \log \frac{M_y^h(t, \omega)}{M_x^h(t, \omega)} \end{aligned} \quad (14)$$

$$\begin{aligned} \hat{\omega}_{xy}(t, \omega) = & \omega + \frac{\frac{\partial}{\partial t} \Phi_x^h(t, \omega) + \frac{\partial}{\partial t} \Phi_y^h(t, \omega)}{2} \\ & + \frac{i}{2} \frac{\partial}{\partial t} \log \frac{M_y^h(t, \omega)}{M_x^h(t, \omega)}. \end{aligned} \quad (15)$$

This shows that the real part of cross-spectrogram reassignment vectors relates to the STFT phases, while the imaginary part relates to the magnitudes. In the case when $x(t) = y(t)$, i.e. in the reassigned spectrogram case, the reassignment

vectors become real-valued and can furthermore be shown to equal the group delay and the instantaneous frequency of the signal, respectively, as demonstrated in for instance [18]. In the same way, in the case when $x(t) \neq y(t)$, the real parts of the cross-spectrogram reassignment vectors relate to the average group delay and instantaneous frequency of $x(t)$ and $y(t)$.

As such, only the real parts of the cross-spectrogram reassignment vectors are used to compute the reassigned cross-spectrogram in (1). Using the facts that $\Re\{-iz\} = \Im\{z\}$, $\Re\{\bar{F}_y^{th}/\bar{F}_y^h\} = \Re\{F_y^{th}/F_y^h\}$, and $\Im\{-\bar{F}_y^{\frac{dh}{dt}}/\bar{F}_y^h\} = \Im\{F_y^{\frac{dh}{dt}}/F_y^h\}$, the following simplified expressions for the cross-spectrogram reassignment vectors are obtained

$$\hat{t}_{xy}^{\text{final}}(t, \omega) = t - \frac{1}{2} \Re \left\{ \frac{F_x^{th}(t, \omega)}{F_x^h(t, \omega)} + \frac{F_y^{th}(t, \omega)}{F_y^h(t, \omega)} \right\} \quad (16)$$

$$\hat{\omega}_{xy}^{\text{final}}(t, \omega) = \omega + \frac{1}{2} \Im \left\{ \frac{F_x^{\frac{dh}{dt}}(t, \omega)}{F_x^h(t, \omega)} + \frac{F_y^{\frac{dh}{dt}}(t, \omega)}{F_y^h(t, \omega)} \right\}. \quad (17)$$

III. SIMULATIONS

In this section, we demonstrate how the reassigned cross-spectrogram can be used to determine phase shifts between frequency-modulated signals and, in particular, how it improves phase estimates in multi-component signals. This is illustrated using simulated data on the following two-component signals

$$x(t) = \Re\{s_1(t) + s_2(t)\} + n_x(t), \quad (18)$$

$$y(t) = \Re\{e^{i\Delta\phi_1} s_1(t) + e^{i\Delta\phi_2} s_2(t)\} + n_y(t), \quad (19)$$

where $t = 1, 2, \dots, 256$, and $\Delta\phi_1$ and $\Delta\phi_2$ are the phase shifts of $s_1(t)$ and $s_2(t)$ in $y(t)$ compared to $x(t)$. The components, $s_1(t)$ and $s_2(t)$, are linear chirps given by

$$s_k(t) = e^{i(\omega_k t + \frac{1}{2} c t^2 + \phi_k)}, \quad k = 1, 2. \quad (20)$$

In all simulations, the chirp rate $c = 20/512$, and the frequency of the first component $\omega_1 = 2\pi 50/512 = 0.6136$. The phases ϕ_k , and phase shifts $\Delta\phi_k$, are uniformly distributed between $-\pi$ and π . Furthermore, two independent white Gaussian noise processes, $n_x(t)$ and $n_y(t)$, were added to the signals. All STFTs were computed with a Gaussian window function, using 512 samples in the FFT. In Fig. 1(a) and (b), the phase shifts of the reassigned cross-spectrogram and the cross-spectrogram for signals in (18) and (19) are exemplified with a signal-to-noise ratio (SNR) equal to 3 dB, where the SNR is defined as the power of one chirp over the noise variance.

In Fig. 1(c), 1000 simulations were made for signals without added noise, with frequency differences $\Delta\omega = \omega_1 - \omega_2$ ranging between 0.1104 and 0.2148, corresponding with 18 to 35 frequency bins. The phase shift of each component $k = 1, 2$ was computed as

$$\Delta\hat{\phi}_k(t) = \arg RS_{xy}^h(t, \eta_k(t)), \quad k = 1, 2, \quad (21)$$

where \arg denotes the argument in $(-\pi, \pi]$, and $\eta_k(t)$ is the estimated TF ridge of component k in the reassigned

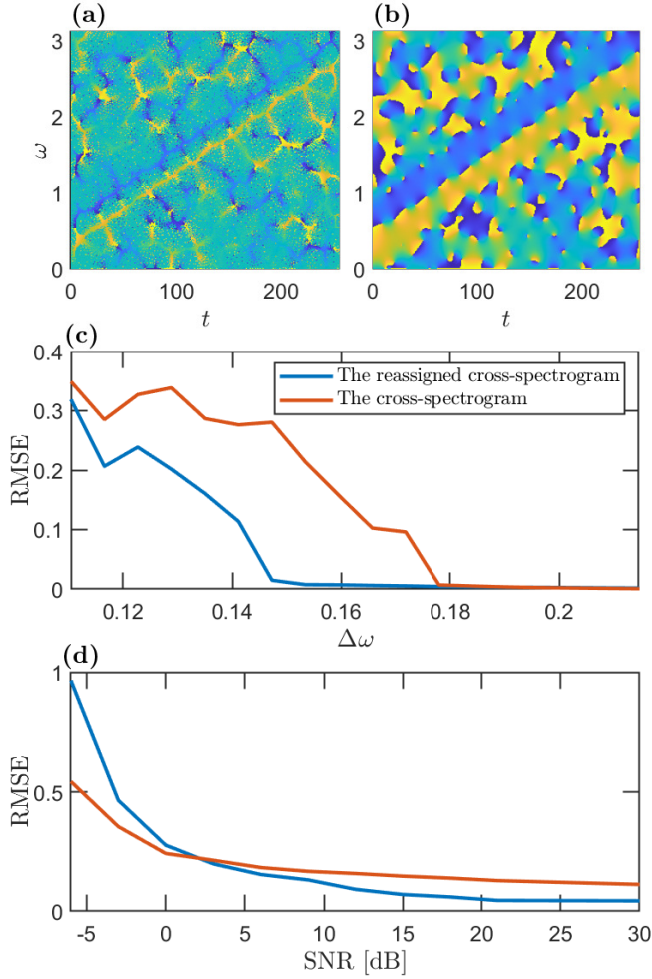


Fig. 1: In a) and b) the phase of the reassigned cross-spectrogram and the cross-spectrogram, respectively. The signals are separated by 25 samples in frequency-direction, such that $\Delta\omega = \omega_1 - \omega_2 = 0.1534$. Furthermore, $\Delta\phi_1 = \pi/2$ and $\Delta\phi_2 = -\pi/2$, and $\text{SNR} = 3\text{dB}$. In c) the lowest possible RMSE of the phase shift estimates is plotted against the frequency distance $\Delta\omega$ between the two signals in the noise-free case. In d), the RMSE is plotted against the SNR of the signals, where $\Delta\omega = 0.1534$ in all simulations.

cross-spectrogram (or cross-spectrogram). MATLAB's function 'tfridge' was used to extract the TF ridges $\eta_k(t)$. This function incorporates a penalty parameter to control for rapid changes in frequency, ensuring smoothness of the extracted ridge. For fairness, the TF ridges were extracted for 10 different penalties logarithmically spaced between 0.01 and 5, and the penalty resulting in the overall smallest root-mean-squared-error (RMSE) is presented in the plot. Due to the periodicity of the phase shift, the square error of the phase

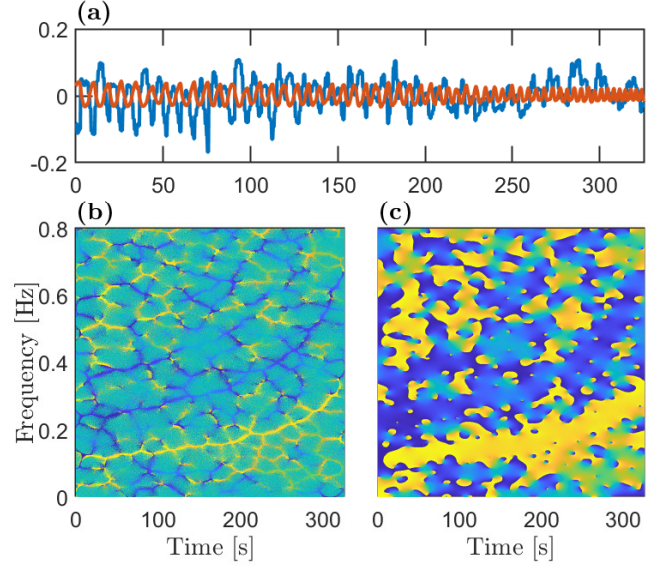


Fig. 2: In a), an HRV-signal centered around zero, and the corresponding respiratory signal, scaled by a factor of five, are shown in blue and orange, respectively. In b) and c), the phase of the reassigned cross-spectrogram and the cross-spectrogram of the signals are shown, respectively.

shift estimates was computed as

$$SE = \frac{1}{2} \sum_{k=1}^2 |\arg e^{i(\Delta\hat{\phi}_k - \Delta\phi_k)}|^2. \quad (22)$$

Because reassignment improves resolution between components, the reassigned cross-spectrogram results in lower RMSE when extracting phase shifts of close components.

In the next simulation, the signals were separated in frequency by $\Delta\omega = 0.1534$, like in Fig. 1(a) and (b), and white Gaussian noise was added to the signals. The phase shifts were extracted in the same way as above, and the smallest possible RMSE for each SNR, based on 1000 simulations, is plotted in Fig. 1(d). For SNR higher than 2 dB, the phase shifts extracted using the reassigned cross-spectrogram remain accurate.

IV. REAL DATA EXAMPLE

Finally, the reassigned cross-spectrogram is exemplified on real data. In this example, we consider the phase-relation between the heart rate variability (HRV) and the respiratory rate of an adult breathing following a metronome during 5 minutes, starting at 0.12 Hz and slowly increasing to 0.35 Hz. More about the data acquisition can be found in [19]. The HRV and respiratory signal are plotted in Fig. 2(a), and the phase of the reassigned cross-spectrogram and cross-spectrogram are shown in Fig. (b) and (c), respectively. At least two chirp-like components, one fundamental frequency and one overtone, are seen in the phase-representations. In both plots, the phase shift

is just below π for the fundamental frequency, and just above $-\pi$ for the overtone.

V. CONCLUSION

In this paper, we have presented novel expressions for the cross-spectrogram reassignment vectors, derived from the cross-quadratic class. Furthermore, we show that the real part of the cross-spectrogram reassignment vectors relates to the phase information of the signals. Because the reassignment technique improves resolution, the reassigned cross-spectrogram is experimentally shown to improve estimates of phase shifts between close signal components. In future research, further improvements of the reassigned cross-spectrogram could be made by incorporating, for instance, higher-order derivatives or multitapers in the reassignment vectors.

APPENDIX

Proof. We find the proof of Lemma 1 by expanding into a double integral using (3)

$$F_x^g(t, \omega) \bar{F}_y^h(t, \omega) = \iint x(\tau_1) \bar{y}(\tau_2) \bar{g}(t - \tau_1) h(t - \tau_2) e^{-i\omega(\tau_1 - \tau_2)} d\tau_1 d\tau_2. \quad (23)$$

Introducing the variables u and τ such that $\tau_1 = u + \tau/2$ and $\tau_2 = u - \tau/2$, the equality can be rewritten as

$$F_x^g(t, \omega) \bar{F}_y^h(t, \omega) = \iint x\left(u + \frac{\tau}{2}\right) \bar{y}\left(u - \frac{\tau}{2}\right) \bar{g}\left(t - u + \frac{\tau}{2}\right) h\left(t - u - \frac{\tau}{2}\right) du d\tau.$$

The integral consists of two parts, one that only depends on the signals, and one that only depends on the windows. The one that depends on the signals can be seen as the *cross-time-lag distribution*

$$r_{x,y}(t, \tau) = x\left(u + \frac{\tau}{2}\right) \bar{y}\left(u - \frac{\tau}{2}\right).$$

The cross-time-lag distribution is connected to the cross-Wigner-Ville distribution through an inverse Fourier transform as

$$r_{x,y}(t, \tau) = \int W_{x,y}(t, \nu) e^{i\nu\tau} \frac{d\nu}{2\pi}. \quad (24)$$

The second part of the expression in (23) is

$$\rho_{g,h}(t - u, \tau) = \bar{g}\left(t - u - \frac{\tau}{2}\right) h\left(t - u + \frac{\tau}{2}\right). \quad (25)$$

Using the expression from equations (24) and (25) we find

$$F_x^g(t, \omega) \bar{F}_y^h(t, \omega) = \iint W_{x,y}(t, \nu) \int \rho_{g,h}(t - u, \tau) e^{-i(\omega - \nu)\tau} d\tau \frac{d\nu}{2\pi}. \quad (26)$$

From this expression, one can introduce the smoothing kernel

$$\begin{aligned} \phi_{g,h}(t - u, \omega - \nu) &= \int \rho_{g,h}(t - u, \tau) e^{-i(\omega - \nu)\tau} d\tau = \\ &= \int \bar{g}\left(t - u + \frac{\tau}{2}\right) h\left(t - u - \frac{\tau}{2}\right) e^{-i(\omega - \nu)\tau} d\tau = \\ &= W_{g,h}(t - u, \omega - \nu). \end{aligned} \quad (27)$$

Finally

$$\begin{aligned} F_x^g(t, \omega) \bar{F}_y^h(t, \omega) &= \\ &= \iint W_{x,y}(t, \nu) W_{g,h}(t - u, \omega - \nu) du \frac{d\nu}{2\pi} = \\ &= \iint W_{x,y}(t - u, \omega - \nu) W_{g,h}(u, \nu) du \frac{d\nu}{2\pi}. \end{aligned} \quad (28)$$

□

REFERENCES

- [1] K. Kodera, C. de Villedary, and R. Gendrin, "A new method for the numerical analysis of nonstationary signals," *Physics of the Earth & Planetary Interiors*, vol. 12, pp. 142–150, 1976.
- [2] F. Auger and P. Flandrin, "Improving the readability of time-frequency and time-scale representations by the reassignment method," *IEEE Trans. on Signal Processing*, vol. 43, pp. 1068–1089, May 1995.
- [3] D. Fourer, F. Auger, and G. Peeters, "Local AM/FM parameters estimation: Application to sinusoidal modeling and blind audio source separation," *IEEE Signal Processing Letters*, vol. 25, no. 10, pp. 1600–1604, 2018.
- [4] F. Auger, E. Chassande-Mottin, and P. Flandrin, "Making reassignment adjustable: The Levenberg-Marquardt approach," in *Proceedings of the ICASSP*. IEEE, 2012, pp. 3889–3892.
- [5] T. Oberlin, S. Meignen, and V. Perrier, "Second-order synchrosqueezing transform or invertible reassignment? towards ideal time-frequency representations," *IEEE Trans. on Signal Processing*, vol. 63, no. 5, pp. 1335 – 1344, 2015.
- [6] M. Hansson-Sandsten and J. Brynolfsson, "The scaled reassigned spectrogram with perfect localization for estimation of Gaussian functions," *IEEE Signal Processing Letters*, vol. 22, no. 1, pp. 100–104, 2015.
- [7] M. Sandsten, J. Brynolfsson, and I. Reinhold, "The matched window reassignment," in *Proceedings of the EUSIPCO*, Rome, Italy, 2018.
- [8] I. Daubechies, J. Lu, and H.-T. Wu, "Synchrosqueezed wavelet transforms: An empirical mode decomposition-like tool," *Applied & Computational Harmonic Analysis*, vol. 30, no. 2, pp. 243 – 261, 2011.
- [9] I. Daubechies, Y. G. Wang, and H.-T. Wu, "ConceFT: concentration of frequency and time via a multitapered synchrosqueezed transform," *Phil. Trans. R. Soc. A*, vol. 374, no. 20150193, 2016.
- [10] M. A. Colominas and S. Meignen, "Adaptive order synchrosqueezing transform," *Signal Processing*, vol. 231, p. 109881, 2025.
- [11] C. K. Kovach, "A biased look at phase locking: Brief critical review and proposed remedy," *IEEE Trans. on Signal Processing*, vol. 65, no. 17, pp. 4468 – 4480, 2017.
- [12] M. Åkesson and M. Sandsten, "Phase reassignment with efficient estimation of phase difference," in *2022 30th European Signal Processing Conference (EUSIPCO)*. IEEE, 2022, pp. 2126–2130.
- [13] O. Keding and M. Sandsten, "Robust phase difference estimation of transients in high noise levels," in *Proceedings of the EUSIPCO*, Belgrade, Serbia, 2022.
- [14] K. C. Meza-Fajardo, "Dispersion analysis of multi-modal waves based on the reassigned cross-s-transform," *Soil Dynamics and Earthquake Engineering*, vol. 143, p. 106610, 2021.
- [15] G. Averbuch, "The spectrogram, method of reassignment, and frequency-domain beamforming," *The Journal of the Acoustical Society of America*, vol. 149, no. 2, p. 747, 2021.
- [16] K. Abratkiewicz, K. Czarnecki, D. Fourer, and F. Auger, "Estimation of time-frequency complex phase-based speech attributes using narrow band filter banks," *2017 Signal Processing Symposium (SPSymposium)*, pp. 1 – 6, 2017.
- [17] F. Auger, E. Chassande-Mottin, and P. Flandrin, "On phase-magnitude relationships in the short-time Fourier transform," *IEEE Signal Processing Letters*, vol. 19, no. 5, pp. 267–270, May 2012.
- [18] K. R. Fitz and S. A. Fulop, "A unified theory of time-frequency reassignment," *arXiv preprint arXiv:0903.3080*, 2009.
- [19] R. Anderson, P. Jönsson, and M. Sandsten, "Insights on spectral measures for HRV based on a novel approach for data acquisition," in *Proceedings of the 40th International Engineering in Medicine and Biology Conference (EMBC)*. Honolulu, HI, USA: IEEE, 2018.